Water Research 200 (2021) 117295

Contents lists available at ScienceDirect

Water Research

journal homepage: www.elsevier.com/locate/watres

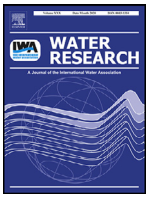

# Seasonal dynamics of the microbial community in two full-scale wastewater treatment plants: Diversity, composition, phylogenetic group based assembly and co-occurrence pattern

Chenxiang Sun[a,b], Bing Zhang[a], Daliang Ning[b], Ya Zhang[b], Tianjiao Dai[a], Linwei Wu[b], Tianle Li[a], Wei Liu[a], Jizhong Zhou[a,b,c], Xianghua Wen[a,*]

[a] Environmental Simulation and Pollution Control State Key Joint Laboratory, School of Environment, Tsinghua University, Beijing 100084, China
[b] Institute for Environmental Genomics and Department of Botany and Microbiology, University of Oklahoma, Norman, OK, 73019, USA
[c] Earth Sciences Division, Lawrence Berkeley National Laboratory, Berkeley, CA, 94720, USA

ARTICLE INFO

*Article history:*
Received 9 November 2020
Revised 20 May 2021
Accepted 21 May 2021
Available online 25 May 2021

*Keywords:*
Microbial community
Assembly
Wastewater treatment plant
Seasonal dynamic

ABSTRACT

The optimal operation and functional stability of a wastewater treatment plant (WWTP) strongly depend on the properties of its microbial community. However, a knowledge gap remains regarding the seasonal dynamics of microbial community properties, especially phylogenetic group based assembly and co-occurrence patterns. Accordingly, in this study, influent and activated sludge (AS) samples were weekly collected from 2 full-scale WWTPs for one year (89 influent and 103 AS samples in total) and examined by high-throughput Illumina-MiSeq sequencing. The results suggested that the microbial community diversity and composition in the influent fluctuated substantially with season, while those in the AS had a relatively more stable pattern throughout the year. The phylogenetic group based assembly mechanisms of AS community were identified by using “Infer Community Assembly Mechanisms by Phylogenetic-bin-based null model (iCAMP)”. The results showed that drift accounted for the largest proportion (52.8%), while homogeneous selection (18.2%) was the most important deterministic process. Deterministic processes dominated in 47 microbial groups (bins), which were also found (~40%) in the AS core taxa dataset. Moreover, the results suggested that *Nitrospira* were more susceptible to stochastic processes in winter, which may provide a possible explanation for nitrification failure in winter. Network analysis results suggested that the network structure of the AS community could be more stable in summer and autumn. In addition, there were no identical keystone taxa found in different networks (constructed from different plants, sources, and seasons), which supported the context dependency theory. The results of this study deepened our understanding of the microbial ecology in AS systems and provided a foundation for further studies on the community regulation strategy of WWTPs.

## 1. Introduction

Wastewater treatment plants (WWTPs), which mostly use the activated sludge (AS) process, play a critical role in the protection of our environment and human health (Ju and Zhang 2015). AS harbors a highly complex microbial community and heavily relies on it for the degradation of organic matter, nutrient removal, and wastewater detoxification (Wagner and Loy 2002). Thus, the functional stability of WWTPs depends largely on the microbial community in AS (Wagner and Loy 2002; Falk; Song et al. 2009; Griffin and Wells 2017; Zhang et al., 2020). Previous studies have revealed the repeated and predictable seasonal patterns of microbial community in natural ecosystems, such as lakes (Shade et al., 2007) and oceans (Fuhrman et al., 2006). For WWTPs, the seasonality of the microbial community in AS has attracted the interest of environmental microbiologists (Griffin and Wells 2017; Johnston and Behrens 2020; Petrovski et al., 2020).

Previously, some researchers performed long-term studies on the dynamics of microbial community structure in AS systems by using different types of conventional molecular tools. For example, by using Terminal Restriction Fragment Length Polymorphism (T-RFLP), successive shifts in AS bacterial community structure were revealed through a weekly sampling campaign for one year (Wells et al., 2011); And, Flowers et al. used automated ribosomal intergenic spacer region analysis (ARISA) to investigate the repeated seasonal pattern of overall community succession in an

---

* Corresponding author.
*E-mail address:* xhwen@tsinghua.edu.cn (X. Wen).

https://doi.org/10.1016/j.watres.2021.117295

enhanced biological phosphorus removal plant throughout a two-year sampling study (Flowers, Cadkin et al. 2013). However, given limitations due to PCR bias or low throughput, the taxonomic information and microbial community diversity could be underestimated.

In recent years, the high-throughput sequencing of 16S rRNA amplicons has greatly deepened our understanding of microbial community dynamics in AS. A previous study indicated that seasonal variation had a stronger impact on the AS bacterial community than any other variation (Zhang et al., 2018). Temperature and dietary habits could be the most important factors leading to community dynamics (Ju et al., 2014; Petrovski et al., 2020). In addition, the dynamics of some key functional groups, such as nitrifying bacteria, were thoroughly investigated in a 55-week sampling campaign (Johnston et al., 2019). Moreover, Jiang et al. highlighted the importance of biotic associations in controlling the bacterial communities in AS (Jiang et al., 2018a); And they captured the high-resolution overall view of community dynamics, especially the bacteria involved in sludge bulking and foaming, by using a long-term and intensively sampled dataset (Jiang et al., 2018b). These studies revealed the detailed dynamic patterns of microbial diversity and community composition in the AS system, which provided a sound foundation for us to explore the dynamics of AS community assembly mechanisms and co-occurrence patterns.

The study of co-occurrence patterns will provide us with new insight into the AS system and improve our understanding of the microbial community beyond those with simple diversity and composition (Jiang et al., 2018b; Shi et al., 2016; Deng et al., 2012). Regarding community assembly mechanisms, there have been intensive debates about this longstanding issue (Tilman 2004; Ning et al., 2020). At present, it is generally accepted that both deterministic processes (including homogeneous selection and heterogeneous selection) and stochastic processes (including homogenizing dispersal, dispersal limitation, and drift) contribute to the assembly of the AS microbial community (Wu et al., 2019; Zhang et al., 2020). However, some studies have reported contrasting results regarding the relative importance of these processes in controlling AS community assembly. Griffin et al. monitored six AS bioreactors for 1 year and found that the communities were highly synchronized at the individual OTU, broad phylogenetic affiliation and community-wide scale. Temperature was the most important driver of the variations in alpha- and beta-diversity; thus, they indicated that the communities were highly controlled by deterministic processes (Griffin and Wells 2017). A similar reactor synchrony was found by Johnston et al. (Johnston et al., 2019). However, recent global survey data (Wu et al., 2019) indicated that stochastic processes were more important in AS community assembly, which was consistent with our previous findings in China (Zhang et al., 2020; Sun et al., 2020). In addition, previous studies have had major limitations because the assembly mechanisms were evaluated at the “whole community” level. However, it was indicated that the actions of the assembly processes were typically at the genotype or population level rather than at the whole community level (Ofiteru et al., 2010; Ning et al., 2020).

Different microorganisms respond differently to environmental changes (such as temperature, SRT, and biodegradability) (Zhang et al., 2020; Sun et al., 2020; Johnston and Behrens 2020); thus, it is reasonable to assume that different “microorganism groups” in AS would possess differentiated assembly mechanisms. However, as only a few studies focus on this topic, there is still a knowledge gap remains regarding the phylogenetic group based AS assembly mechanisms. Recently, Ning et al. proposed a new framework named Infer Community Assembly Mechanisms by Phylogenetic-bin-based null model (iCAMP), which considers assembly mechanisms at the level of individual taxa/lineages rather than the whole community (Ning et al., 2020). iCAMP showed high accuracy and sensitivity on a simulated community, and it showed high effectiveness and robustness in grassland microbial communities (Ning et al., 2020). This framework provides us with a powerful tool to investigate the assembly mechanisms of different microorganism groups in the AS system.

In this study, influent and AS samples were weekly collected from two full-scale WWTPs for one year (89 influent and 103 AS samples in total). High-throughput 16S rRNA gene amplicon sequencing and multiple bioinformatics methods were used to reveal the seasonal dynamics of microbial community diversity, composition, phylogenetic group based assembly, and co-occurrence patterns. This study will help to deepen our understanding of the microbial ecology in AS systems, and it provides a foundation for further studies on the community regulation strategy of WWTPs.

## 2. Materials and methods

### *2.1. WWTPs and sampling*

Influent and AS samples were collected between January 2015 and January 2016 from two full-scale WWTPs (abbreviated as GBD and BXH) in Beijing, China. GBD primarily treats municipal wastewater with a capacity of 1,000,000 $m^3$ per day for a population of ~2,400,000 people. It employs an anaerobic/anoxic/aerobic (A/A/O) process with the sludge retention time (SRT) of approximately 10 days. BXH treats mainly municipal wastewater with a capacity of 100,000 $m^3$ per day to provide reclaimed water to Olympic venues and the Olympic park. It uses a A/A/O+membrane bioreactor (MBR) process with the SRT of about 17 days.

A total of 89 influent samples (46 from GBD and 43 from BXH) and 103 AS samples (52 from GBD and 51 from BXH) were collected at 52 time points. For each weekly influent sample, 200 ml of liquid was collected in four 50-ml sterile tubes. For each weekly AS sample, 50 ml of liquid was collected from the inlet and outlet zones of the aeration tank, and combined as a single time point AS sample. Temperature, pH, conductivity and dissolved oxygen (DO) of the influent and AS samples were determined in situ by using a multi-parameter water quality measuring instrument (Thermo Orion 4-Star, Thermo Fisher Scientific, MA, USA). All of the collected samples were briefly precipitated in situ for 30 min to decant the supernatant, and immediately transported to the laboratory on ice within 2 h. Each 100 ml of influent sample and each 2 ml of AS sample were centrifuged at 15,000 g for 20 min and 15,000 g for 10 min, respectively. The supernatant of the influent and AS samples was decanted, and the pellets were stored at −80 °C until the DNA was extracted. Chemical oxygen demand (COD), ammonia-N, nitrite-N, nitrate-N, total nitrogen (TN), and total phosphorus (TP) were determined for both influent and AS samples. Mixed liquor suspended solids (MLSS) and mixed liquor volatile suspended solids (MLVSS) were additionally determined for AS samples. All of these parameters were measured following the standard methods (ChineseNEPA 2002) within 24 h after sample collection.

### *2.2. DNA extraction, illumina sequencing, and data accession*

Microbial genomic DNA was extracted by PowerSoil DNA isolation kit (MoBio Laboratories, Carlsbad, CA, USA) according to the manufacturer's instructions. Then, the quality of extracted DNA was examined by a ND-2000 spectrophotometer (Nanodrop Inc., Wilmington, DE, USA). DNA with the A260/A280 ratio between 1.8–2.0, and the A260/A230 ratio higher than 1.7 was used for sequencing. The variable region 4 (V4) of the 16S rRNA gene was amplified using the forward primer 515F (5′-GTGCCAGCMGCCGCGGTAA-3′) and the reverse primer 806R (5′-GGACTACHVGGGTWTCTAAT-3′).

An effective and robust two-step PCR was used to amplify the sequences (Wu et al., 2019; Zhang et al., 2020). The detailed sequencing process was summarized in Text S1. The sequencing data generated in this study were deposited into the National Center for Biotechnology Information (NCBI, https://submit.ncbi.nlm.nih.gov) database with the accession number PRJNA625560.

### 2.3. Sequence processing and data analyses

Raw sequences were processed by the galaxy platform of the Institute for Environmental Genomics (IEG) Statistical Analysis Pipeline (http://ieg3.rccc.ou.edu:8081/). The detailed sequence processing procedure was summarized in Text S2. After assembling and quality filtering, a total of 9,151,618 high-quality sequences were obtained from the whole sequencing dataset, which were clustered into 33,411 operational Taxonomic units (OTUs). To reduce errors and perform a relatively fair comparison among all samples, the sequence number in each sample was rarefied to the same depth (30,000 sequences per sample), except for four samples (2 influent samples and 2 AS samples). For these four samples, unrarefied sequences were retained (Table S2).

All 192 samples were divided into 16 groups based on different seasons (spring, March – May; summer, June – August; autumn, September – November; winter, December - February), different plants (GBD and BXH) and different sources (influent and AS). These groups were abbreviated as: 1) samples from the influent of GBD in different seasons: GBD_Inf_Spr, GBD_Inf_Sum, GBD_Inf_Aut, and GBD_Inf_Win; 2) samples from the activated sludge of GBD in different seasons: GBD_AS_Spr, GBD_AS_Sum, GBD_AS_Aut, and GBD_AS_Win; 3) samples from the influent of BXH in different seasons: BXH_Inf_Spr, BXH_Inf_Sum, BXH_Inf_Aut, and BXH_Inf_Win; and 4) samples from the activated sludge of BXH in different seasons: BXH_AS_Spr, BXH_AS_Sum, BXH_AS_Aut, and BXH_AS_Win. Permutational multivariate analysis of variance (PERMANOVA) was used to test the differences among groups.

Richness, Shannon-Wiener (H) and inverse Simpson indices were used to evaluate the alpha diversity of the microbial communities; Pielou's (J) index was used to investigate the evenness of the microbial communities. To identify the seasonal community succession patterns, the relative abundance data of all samples were ordinated by nonmetric multidimensional scaling (NMDS) analysis with Bray-Curtis distance. The microbial community composition was visualized by Circos (Krzywinski et al., 2009). The diversity indices, NMDS, dissimilarity matrix, and Mantel test were performed in R (version 3.4.4) using the vegan package (Dixon 2003, version 3.2). The Infer Community Assembly Mechanisms by Phylogenetic-bin-based null model (iCAMP) was used to investigate the assembly mechanisms of different microorganism groups (Ning et al., 2020). The R code for iCAMP was available as an open-source R package, "iCAMP", which can be downloaded from the Comprehensive R Archive Network (CRAN, https://cran.r-project.org/). And, the custom scripts for iCAMP were available from GitHub (https://github.com/DaliangNing/iCAMP1). By using iCAMP, five assembly mechanisms of different microorganism groups (called 'bins') were identified, including homogeneous selection (HoS), heterogeneous selection (HeS), dispersal limitation (DL), homogenizing dispersal (HD), and drift (DR). A detailed explanation of these mechanisms can be found in a previous study (Zhou and Ning 2017). Besides, the seasonality-induced changes in HoS and DR were investigated in this study, and a change was defined as a positive value if the relative contribution of HoS or DR was higher in summer than in winter.

Microbial ecological networks were constructed by using the Molecular Ecological Network Analysis Pipeline (MENAP) (http://ieg2.ou.edu/MENA/) to reveal the possible co-occurrence patterns among microorganisms (Zhou et al., 2010; Deng et al., 2012). During the network construction procedure, only those OTUs detected in more than 85% of the samples were kept to eliminate unrepresentative OTUs and reduce complexity. To identify the keystone taxa, the following simplified classification was established: (i) peripheral nodes (Zi $\le$ 2.5, Pi $\le$ 0.62; i.e., "Zi" indicates within-module connectivities and "Pi" indicates among-module connectivities), which possessed only a few links that were almost always associated with nodes within their modules; (ii) connectors (Zi $\le$ 2.5, Pi $>$ 0.62), which were highly connected to several modules; (iii) module hubs (Zi $>$ 2.5, Pi $\le$ 0.62), which were highly connected to numerous microbes in their own modules; and (iv) network hubs (Zi $>$ 2.5, Pi $>$ 0.62), which acted as both module hubs and connectors. For each network, 100 corresponding random networks were generated with the same network size and average number of links. The Z-test was then used to investigate the differences in the topological parameters between the constructed networks and the random networks to ensure that the ecological networks were non-random.

## 3. Results and discussion

### 3.1. Seasonal dynamics of microbial community diversity

It was demonstrated that the functions and stability of wastewater treatment systems were determined by the diversity and composition of AS communities (Jousset et al., 2017), and WWTPs with higher alpha diversity could be more stable (Sun et al., 2020; Zhang et al., 2020). To determine how the alpha diversity of AS and influent communities changed across seasons, key diversity indices of these samples including richness, Shannon-Wiener index (H), Pielou's evenness index (J), and inverse Simpson's index, were calculated to reveal their seasonal dynamic patterns. As shown in Fig. 1, richness represented the number of observed species and ranged from 904 (GBD_Inf_Spr) to 5606 (GBD_Inf_Aut) in these samples. The Shannon-Wiener index considering both the richness and relative abundance of each species varied from 2.90 (BXH_Inf_Spr) to 7.32 (GBD_Inf_Aut) in these time series samples. Besides, the Pielou's evenness index ranged from 0.40 (BXH_Inf_Spr) to 0.85 (GBD_Inf_Aut), and the inverse Simpson diversity index varied from 3.46 (BXH_Inf_Spr) to 284.53 (BXH_Inf_Spr).

The results showed that the microbial diversity of influent samples fluctuated dramatically across time points. Moreover, the maximum and minimum values of each index all appeared in influent samples. For example, the maximum and minimum values of the inverse Simpson diversity index all occurred in BXH spring influent samples. This result was not surprising because the characteristics of influent wastewater are related to people's living habits (such as eating habits and shower frequency) and production activities in different seasons, which are not subject to artificial control and fluctuate frequently (Martin and Vanrolleghem 2014; Chen et al., 2019; Petrovski et al., 2020). Thus, the microbial community could be affected by dramatic changes in substrates, such as COD (Mantel test, $R = 0.205$, $P < 0.001$) and nitrate-N (Mantel test, $R = 0.509$, $P < 0.001$). While in AS samples, the microbial diversity was relatively stable in different seasons. Here, the WWTPs performance was also determined. As shown in figures S1 – S3, the system performance was relatively stable in terms of COD, ammonia-nitrogen and total nitrogen removal, and almost all of the effluent quality indices met the discharge standard during the sampling period. The performance of these two full-scale WWTPs was generally stable throughout the year, which may partially be attributed to the relatively stable microbial diversity in AS. However, the diversity of the AS community in summer was still significantly higher than that in winter ($t$-test; GBD, $P < 0.01$; BXH, $P < 0.05$). Previous studies indicated that temperature was an important driver of repeat-

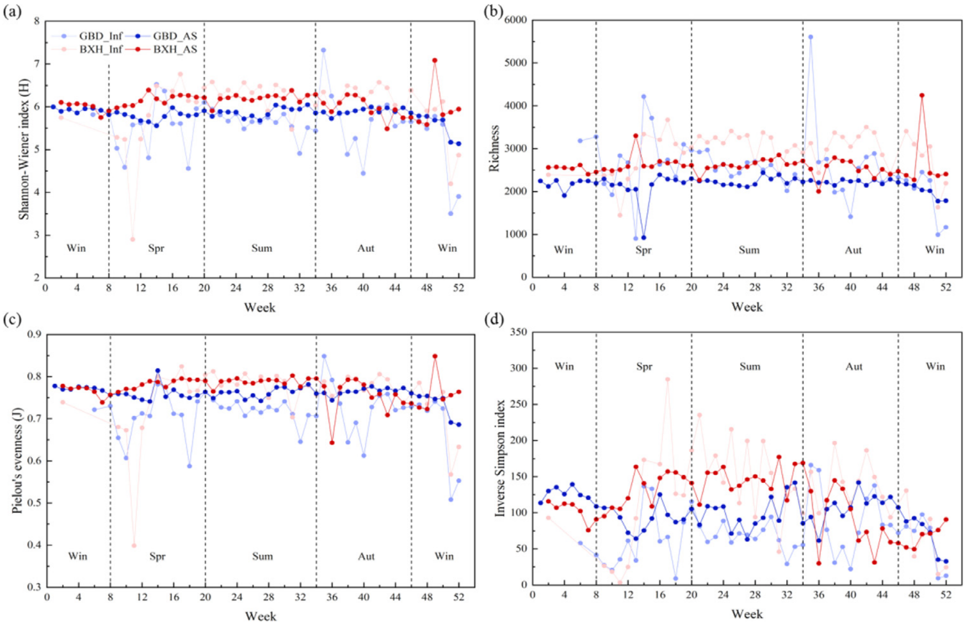

**Fig. 1.** Seasonal dynamic patterns of a) Shannon-Wiener (H) index; b) Richness; c) Pielou's evenness (J) index; and d) Inverse Simpson index. GBD_Inf and BXH_Inf represent the influent of GBD and BXH; GBD_AS and BXH_AS represent the activated sludge of GBD and BXH.

able seasonal alpha diversity patterns accompanied by population synchrony and shifts in broad phylogenetic abundance (Flowers, Cadkin et al. 2013; Griffin and Wells 2017). In this study, a similar sinusoidal temperature pattern was also observed (figure S4). Therefore, the significant difference in AS microbial diversity between summer and winter could be at least partly attributed to the changes in temperature (Mantel test, $R = 0.289$, $P < 0.001$). Collectively, these results suggested that the microbial diversity in the influent fluctuated substantially with season, while AS had a relatively more stable diversity pattern throughout the year.

### 3.2. Seasonal dynamics of microbial community composition

To better understand the structure of microbial community, the taxonomic affiliation at the phylum or class (for Proteobacteria) level was visualized by Circos (Fig. 2, figure S5–7). Firmicutes, Bacteroidetes, Beta-, Gamma-, and Epsilon-proteobacteria were the most dominant phyla (or classes) in the influent samples. In addition, the composition of influent communities varied greatly in different seasons, which may be attributed to sharp fluctuations in the influent characteristics (Martin and Vanrolleghem 2014; Zheng et al., 2019; Petrovski et al., 2020). In the AS community, the composition was more seasonally stable than that in the influent community. Consistent with previous studies (Xia et al., 2018; Sun et al., 2020), the most dominant phyla (or classes) in the AS community were Alpha-, Beta-, Gamma-, Delta-proteobacteria, Actinobacteria, Acidobacteria, Chloroflexi, Nitrospirae, and Planctomycetes. However, even though the composition of AS community was similar in different seasons, the results of PERMANOVA suggested significant ($P < 0.001$) differences among them. As shown in Table S3, there were significant differences among almost all groups, except for some influent groups ($P > 0.05$). The results suggested that the AS community might have seasonal succession patterns. Therefore, to explore the overall community dynamics, the community data were ordinated by NMDS. As shown in Fig. 3, all samples were clearly clustered into four groups: GBD influent, GBD activated sludge, BXH influent and BXH activated sludge. The results showed that there were significant differences between the influent and AS communities. Moreover, the distance between GBD_Inf and BXH_Inf was closer than that of GBD_AS and BXH_AS, indicating that the difference between the AS community was greater than that of the influent community, which could be related to the different wastewater treatment processes. In addition, there were no seasonal succession patterns in influent communities, but a continual succession was found (i.e., the continuous variation of influent samples in the NMDS figure), which could be attributed to the irregular changes in influent characteristics. While in AS communities, a clear seasonal succession pattern of microbial community structure was found (i.e., the communities from spring and winter were closer in the NMDS figure), which was due to the similar organic and nutrient removal functions performed by the AS systems throughout the year. As indicated by previous studies, seasonal variation would only shift the microbial community structures, but not enough to change the functional genes (Griffin and Wells 2017; Liu et al., 2019). Besides, as one of the most important factors influencing the community structure, temperature ($P < 0.001$) was more similar in winter and spring (Figure S4). Thus, it was reasonable that AS communities exhibited seasonal succession patterns.

To understand which microorganisms were responsible for the differences in the seasonal AS community, the top 50 dominant genera (accounting for 20.8% - 73.7% of the relative abundance) were investigated. Besides, their putative functions were identified by using the MiDAS 3 database (Nierychlo et al., 2020). As shown in figure S8, the abundance of some genera was significantly different among seasons. For example, for the top 15 genera, the abundances of *Ferruginibacter* ($P < 0.001$), *Nitrospira* ($P < 0.001$), *Dechloromonas* ($P < 0.001$), *Zoogloea* ($P < 0.01$), *Aridibacter* ($P < 0.001$), *Phaeodactylibacter* ($P < 0.001$), and *Gemmobacter* ($P < 0.001$) were significantly different between summer and winter, whereas *Terrimonas, Dokdonella, Nitrosomonas, Chryseolinea, Lewinella, Arenimonas, Comamonas*, and *Gp4* had no significant differences. The in situ physiology of *Ferruginibacter* in activated sludge has not been determined (Nierychlo et al., 2020). And, *Aridibacter* were reported to metabolize a variety of monomeric sugars, organic acids, and complex proteinaceous substrates in wastewater (Nierychlo et al., 2020). *Nitrospira* are considered to be the most common and abundant Nitrite oxidizing bacteria (NOB) in WWTPs (Daims et al., 2001), and *Dechloromonas* are able to assim-

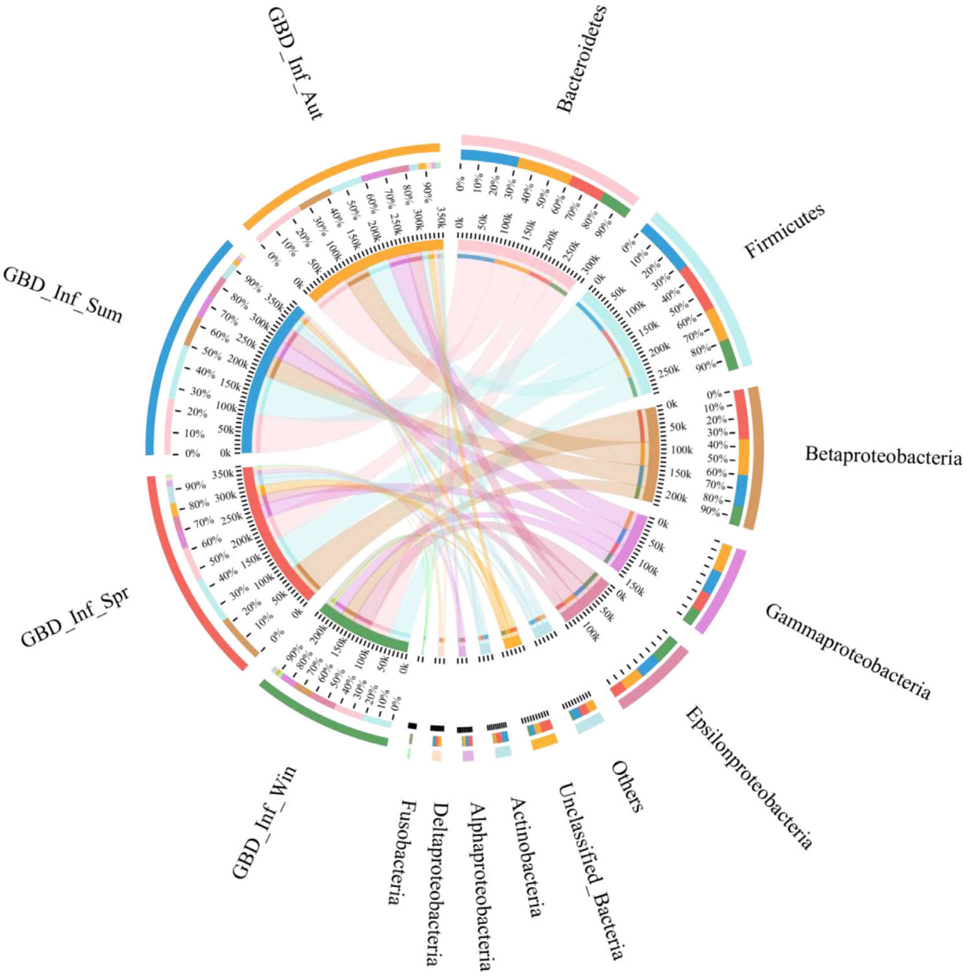

**Fig. 2.** Circular representation of seasonal microbial community composition at phylum or class (for Proteobacteria) level in GBD influent. The outmost two circles list the names of each group and each phylum (or class). The width of the connecting line on the outer ring represents the percentages of microorganisms in these groups (left side of the diagram) and correlates the relative abundance of different taxonomies (right side of the diagram). The microbial phyla (or classes) which relative abundance were lower than 2% were combined as “others”.

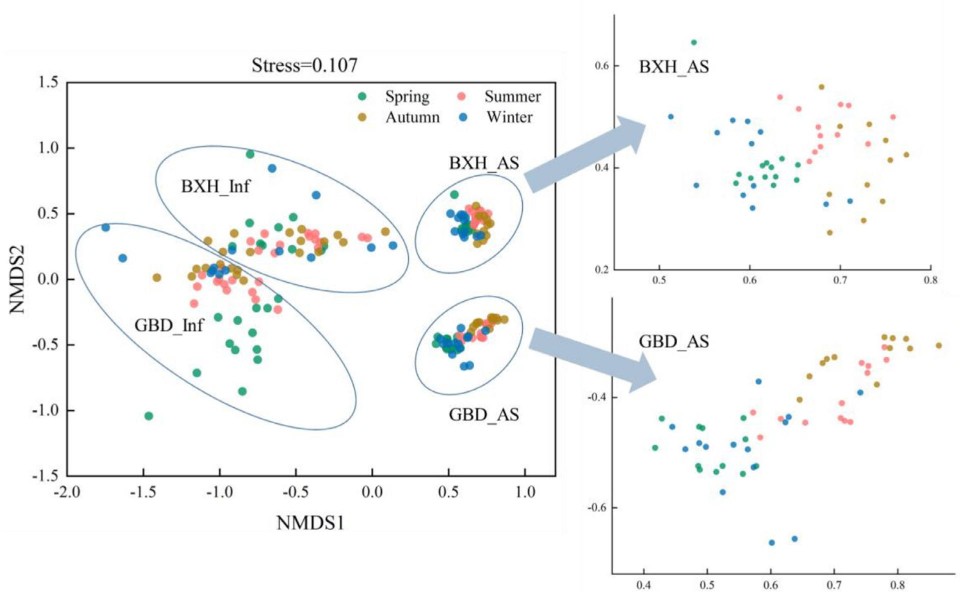

**Fig. 3.** Nonmetric Multidimensional Scaling (NMDS) analysis of seasonal microbial community dynamics. “GBD” and “BXH” represent two different full-scale WWTPs; “Inf” and “AS” represent influent and activated sludge, respectively. “Spr”, “Sum”, “Aut” and “Win” represent spring, summer, autumn, and winter, respectively.

ilate VFAs with nitrite as the electron acceptor under anoxic conditions playing a role in denitrification (Ginige, Keller et al. 2005; McIlroy et al., 2016). However, even though the abundance of *Nitrospira* and *Dechloromonas* was significantly different between seasons, the nitrogen removal performance of full-scale WWTPs was relatively stable throughout the year (figure S3), indicating that there might have been nitrogen removal functional redundancy in the system. Besides, *Zoogloea* were the abundant denitrifier in AS system, and its overgrowth suggested the occurrence of non-viscous bulking (Larsen et al., 2008). Therefore, the significantly higher abundance of *Zoogloea* may suggest higher risks of sludge bulking in winter. In summary, the results here revealed the dominant phyla (or classes) in influent and AS samples, the seasonal succession patterns of AS community, and the seasonal dynamics of dominant genera in AS samples.

### *3.3. Assembly mechanisms across different phylogenetic groups in AS*

Given that the microbial diversity and community composition were seasonally dynamic, we further investigated the driving forces that shaped the community structure, i.e., the community assembly mechanisms. The community assembly mechanism is one of the most compelling questions in ecology, and it is the theoretical basis for regulation of the AS community via the operational parameters of WWTPs (Zhou and Ning 2017; Zhang et al., 2020; Ning et al., 2020). Previous studies have indicated that assembly mechanisms mainly include deterministic and stochastic processes. The deterministic processes were divided into homogeneous selection (HoS) and heterogeneous selection (HeS), while the stochastic processes included dispersal limitation (DL), homogenizing dispersal (HD), and drift (DR) (Zhou and Ning 2017). The whole community based AS assembly mechanism studies have demonstrated some controversy, especially in answering the question of whether deterministic or stochastic processes are predominant; And, based on these controversial results (Griffin and Wells 2017; Johnston et al., 2019; Wu et al., 2019), we hypothesized that some phylogenetic groups were under strong selection, whereas others could be under strong drift. However, this type of difference cannot be discerned by whole-community based metrics. In this study, the assembly mechanisms of different microorganism groups (called “bins”) in AS were investigated by using our newly developed tool – iCAMP (Ning et al., 2020). To the best of our knowledge, this is the first attempt to distinguish the assembly mechanisms of different microorganisms in AS.

The 33,411 observed OTUs were divided into 337 phylogenetic bins, and the assembly mechanisms of these bins were shown in Fig. 4. More detailed information can be found in Supplementary 2. Overall, drift accounted for the largest proportion of the assembly mechanisms (DR, 52.8%), followed by dispersal limitation (DL, 22.1%) and homogeneous selection (HoS, 18.2%), while homogenizing dispersal (HD, 5.3%) and heterogeneous selection (HeS, 1.6%) accounted for smaller proportions. The deterministic processes dominated in 47 bins (13.9% of the bin numbers and 36.3% of the relative abundance), and the stochastic processes dominated in 290 bins (86.1% of the bin numbers and 63.7% of the relative abundance). Drift was found to be the most important stochastic process and is referred to as an inherent stochastic process encompassing birth, death, and reproduction (Zhou and Ning 2017). The results indicated the importance of stochastic processes in shaping the AS microbial community with an average stochasticity of approximately 75%, and this value was very similar to the global survey data published by the Global Water Microbiome Consortium (Wu et al., 2019). We further investigated these stochastic-predominant bins. Most of them were affiliated to Proteobacteria (37.2%, mainly alpha-, beta-, gamma-, and delta-proteobacteria), Firmicutes (12.1%), Bacteroidetes (10.0%), Actinobacteria (7.2%), and Acidobacteria (4.5%). WWTPs are inherently open systems (Ofiteru et al., 2010) that continuously receive wastewater, which favors microorganism immigration from the influent. Influent is an important source for the AS community (McLellan et al., 2010; Zheng and Wen 2019). And, some non-growing bacteria which entering the system with influent may also had influence on the AS community, as previously demonstrated for anaerobic digesters in WWTPs (Jiang et al., 2021). Thus, it is not surprising that so many phylogenetic groups in AS were primarily influenced by stochastic processes. Many long-term studies have found that the community structure is affected by short-term appeared OTUs (called ‘transient/intermediate taxa’) (Jiang et al., 2018b; Johnston et al., 2019; Zheng and Wen 2019). We speculated that these short-term appeared OTUs were mainly influenced by stochastic processes; however, more data are needed to support this hypothesis.

Deterministic processes, mainly homogeneous selection, were predominant in 47 bins. Homogeneous selection refers to selection under homogeneous abiotic and biotic environmental conditions leading to more similar structures among communities (Zhou and Ning 2017). The results here indicated that these bins were selected under the selection pressure of WWTPs. The taxonomic information of these 47 bins was summarized in table S4. Overall, they were mostly affiliated to Actinobacteria, Alpha-Proteobacteria, Firmicutes, Bacteroidetes, and Nitrospirae. Then, the putative functions of these bins were identified by the MiDAS 3 database (Nierychlo et al., 2020). As shown in Fig. 5, most of them (22 out of 47) were aerobic heterotrophs, indicating that they may play an important role in organic degradation and nutrient removal. Chemoautotrophs or mixtrophs were also observed. Seven out of 47 bins were identified as positive or variable for nitrite reduction, indicating that they were putative denitrifiers (Nierychlo et al., 2020). NOB, Phosphorus accumulating organisms (PAO), and Glycogen accumulating organisms (GAO) were also observed in these deterministic-predominant bins; however, there were very few of them. As shown in Fig. 5, most metabolic properties of these bins were not assessed. We believe that these microorganism groups, which can be selected by the deterministic processes in WWTPs, are of great significance and may be the basis for future regulation of activated sludge communities. Further researches are needed to identify their functions.

Based on the frequency and relative abundance, the core taxa in AS have been studied on spatial (Saunders et al., 2016; Wu et al., 2019) or temporal scales (Griffin and Wells 2017; Jiang et al., 2018a). However, some inconsistencies still exist. Twenty-eight OTUs were defined as the core bacterial community in our previous global survey, in which *Nitrospira* was the most important NOB (Wu et al., 2019). Nonetheless, a recently published study found that there were no members of the genus *Nitrospira* in the studied system, and the authors extended the definition of the core microbiome (Johnston and Behrens 2020). To some extent, the definition of “core taxa” was “plant-specific”. Besides, a previous study suggested that there should be no shared taxa between WWTPs if the sampling period was long enough (Jiang et al., 2018a). Nevertheless, we still hypothesized that there were core taxa in WWTPs, considering that the WWTPs performed similar nutrient removal functions anywhere and at any time. Moreover, we further hypothesized that the assembly mechanisms of these core taxa should be deterministically dominated. In this way, they can exist under the selection pressure of WWTPs. To test this hypothesis, two local core taxa datasets were collated. As shown in table S5, the dataset 1 contains 29 core taxa (relative abundance $> 0.1\%$ and frequency $> 80\%$) of our large-scale spatial AS samples (Zhang et al., 2020) and temporal AS samples (this study) from China; dataset 2 contains the core taxa (28 OTUs) of our previous global survey (Wu et al., 2019). As shown in Fig. 5, 19 out of 47 (~40%)

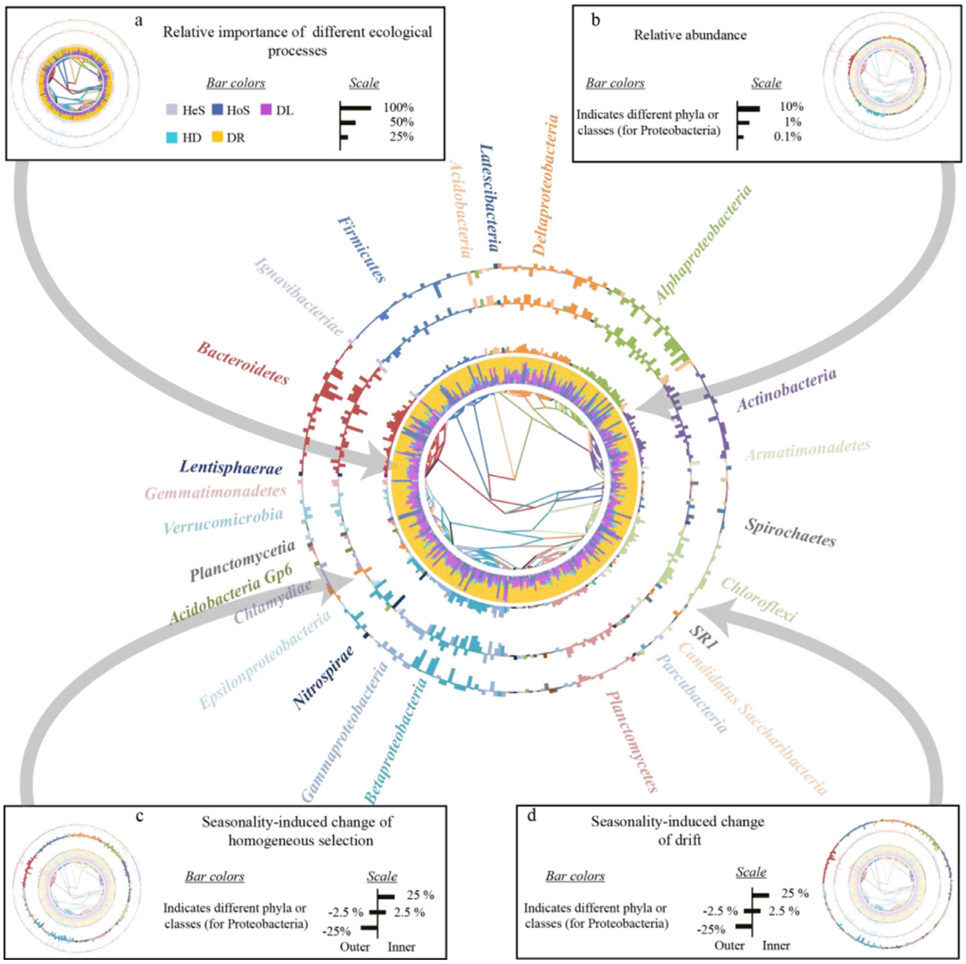

**Fig. 4.** Assembly mechanisms across different phylogenetic groups (bins) in AS. The phylogenetic tree was displayed at the center. a, the relative importance of different ecological processes in each bin (stacked bars in first annulus), and the legend was shown at upper left. Homogeneous selection (HoS), heterogeneous selection (HeS), dispersal limitation (DL), homogenizing dispersal (HD), and drift (DR); b, relative abundance of each bin (second annulus); c, seasonality-induced change of homogeneous selection (third annulus); d, seasonality-induced change of drift (fourth annulus). It is defined as a positive value if the relative contribution of HoS or DR is higher in summer than it in winter.

deterministic-dominated bins were found in core taxa dataset 1 or 2. In addition, 14 out of 47 bins were found in dataset 1, and 8 out of 47 bins were found in dataset 2. There were 3 bins found in both dataset 1 and 2: bin 248, bin 285, and bin 289, and their taxonomic information was summarized in table S4. Bin 248 was identified as *Nitrospira*, which is considered to be the most common and abundant NOB in WWTPs (Nierychlo et al., 2020). Bin 285 was identified as *Dokdonella*, which is only known as an aerobic heterotroph, and its in situ functions have not been studied (Nierychlo et al., 2020). Bin 289 was identified as *Sideroxydans* (affiliated to family Comamonadaceae), which is little known to us. On the whole, the results here suggested that approximately 40% of the deterministic-dominated bins were the core taxa in WWTPs, and they might contribute to AS functions. Future studies are needed to investigate whether and how we can use these bins to regulate the AS community and functions of WWTPs.

As mentioned above, HoS was the main contributor to deterministic processes, while DR accounted for the largest proportion of stochastic processes. Thus, as shown in Fig. 4(c) and (d), we further investigated the seasonal changes in HoS and DR. Overall, the HoS and DR process were significantly different between summer and winter (*t*-test, $P < 0.001$). There were 136 out of 337 bins that had higher DR in winter than summer (the negative/outer value in figure), while 134 out of 337 bins showed higher HoS in summer (the positive/inner value in figure). Previous studies have revealed that seasonality significantly influences the microbial diversity and community composition in AS, and in this study, the results suggested that the assembly mechanisms were also affected by seasonality. It is worth noting that *Nitrospira* showed a lower HoS in winter, and the seasonality-induced change in HoS was 25.7%. The results suggested that *Nitrospira* were more susceptible to stochastic processes in winter, which may affect population abundance. Considering that nitrification failure mainly occurs in winter (Johnston et al., 2019), the results here may provide a possible explanation from the assembly mechanism perspective.

### *3.4. Seasonal dynamics of microbial co-occurrence patterns*

As one of the deterministic processes, microbial co-occurrence patterns were reported to be the most important driver shaping community assembly (Ju and Zhang 2015). Accordingly, 16 networks were constructed with the same threshold value of 0.990. It was suggested that the network structures were non-random and unlikely to appear due to chance, as indicated by the significant differences between empirical networks and their 100 corresponding random networks, which had identical network sizes and average number of links (Table S6– S21). As shown in Fig. 6, Tables 1 and 2, the influent networks differed greatly from the AS networks, especially in spring and winter. Influent assemblages formed larger networks with more nodes and links than AS networks, which in-

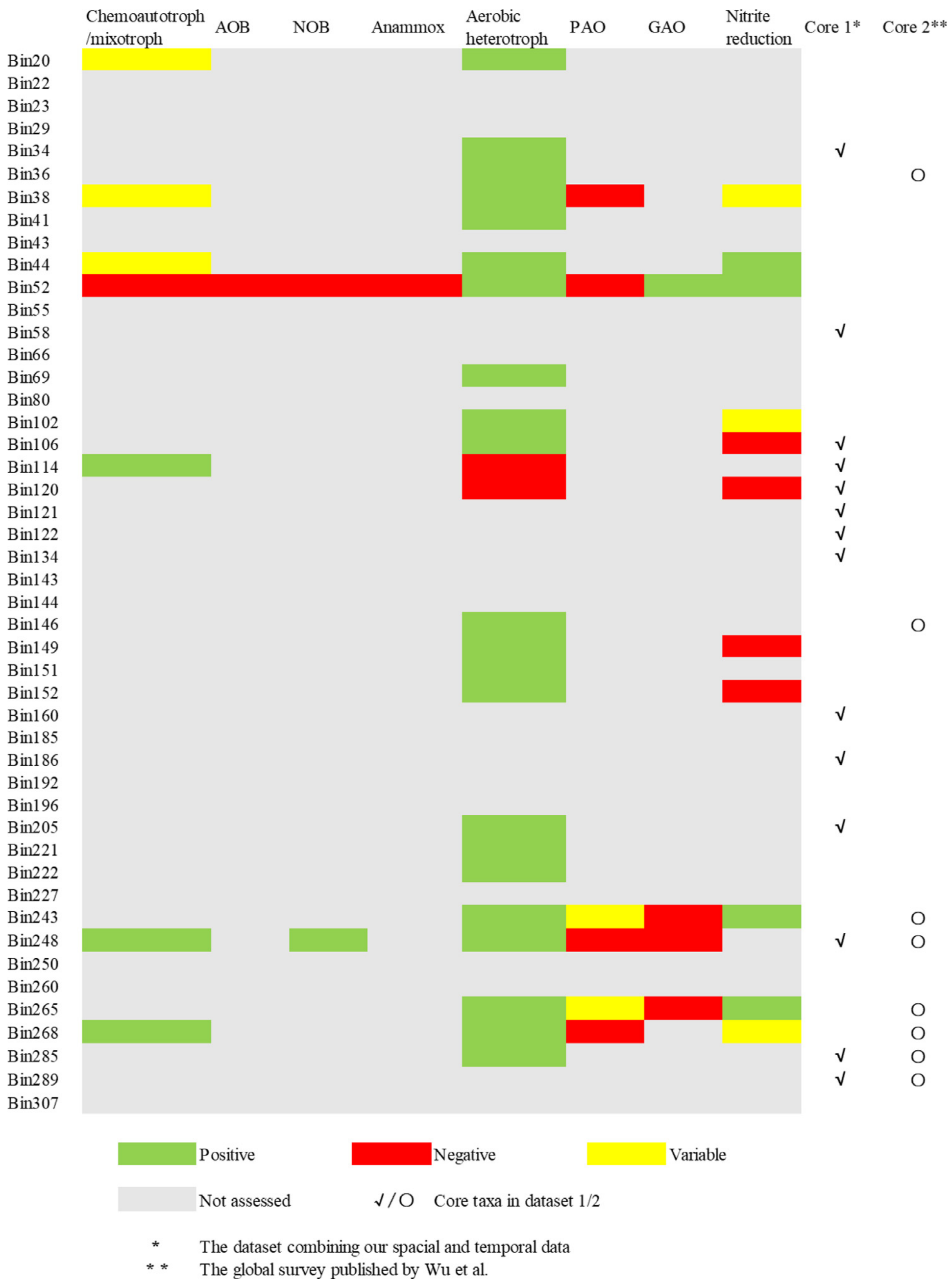

| | Chemoautotroph /mixotroph | AOB | NOB | Anammox | Aerobic heterotroph | PAO | GAO | Nitrite reduction | Core 1* | Core 2** |
|---|---|---|---|---|---|---|---|---|---|---|
| Bin20 | 🟨 | | | | 🟩 | | | | | |
| Bin22 | | | | | | | | | | |
| Bin23 | | | | | | | | | | |
| Bin29 | | | | | | | | | | |
| Bin34 | | | | | 🟩 | | | | √ | |
| Bin36 | | | | | 🟩 | | | | | O |
| Bin38 | 🟨 | | | | 🟩 | 🟥 | | 🟨 | | |
| Bin41 | | | | | 🟩 | | | | | |
| Bin43 | | | | | | | | | | |
| Bin44 | 🟨 | | | | 🟩 | | | 🟩 | | |
| Bin52 | 🟥 | 🟥 | 🟥 | 🟥 | 🟩 | 🟥 | 🟩 | 🟩 | | |
| Bin55 | | | | | | | | | | |
| Bin58 | | | | | | | | | √ | |
| Bin66 | | | | | | | | | | |
| Bin69 | | | | | 🟩 | | | | | |
| Bin80 | | | | | | | | | | |
| Bin102 | | | | | 🟩 | | | 🟨 | | |
| Bin106 | | | | | 🟩 | | | 🟥 | √ | |
| Bin114 | 🟩 | | | | 🟥 | | | | √ | |
| Bin120 | | | | | 🟥 | | | 🟥 | √ | |
| Bin121 | | | | | | | | | √ | |
| Bin122 | | | | | | | | | √ | |
| Bin134 | | | | | | | | | √ | |
| Bin143 | | | | | | | | | | |
| Bin144 | | | | | | | | | | |
| Bin146 | | | | | 🟩 | | | | | O |
| Bin149 | | | | | 🟩 | | | 🟥 | | |
| Bin151 | | | | | 🟩 | | | | | |
| Bin152 | | | | | 🟩 | | | 🟥 | | |
| Bin160 | | | | | | | | | √ | |
| Bin185 | | | | | | | | | | |
| Bin186 | | | | | | | | | √ | |
| Bin192 | | | | | | | | | | |
| Bin196 | | | | | | | | | | |
| Bin205 | | | | | 🟩 | | | | √ | |
| Bin221 | | | | | 🟩 | | | | | |
| Bin222 | | | | | 🟩 | | | | | |
| Bin227 | | | | | | | | | | |
| Bin243 | | | | | 🟩 | 🟨 | 🟥 | 🟩 | | O |
| Bin248 | 🟩 | | 🟩 | | 🟩 | 🟥 | 🟥 | | √ | O |
| Bin250 | | | | | | | | | | |
| Bin260 | | | | | | | | | | |
| Bin265 | | | | | 🟩 | 🟨 | 🟥 | 🟩 | | O |
| Bin268 | 🟩 | | | | 🟩 | 🟥 | | 🟨 | | O |
| Bin285 | | | | | 🟩 | | | | √ | O |
| Bin289 | | | | | | | | | √ | O |
| Bin307 | | | | | | | | | | |

🟩 Positive 🟥 Negative 🟨 Variable

▨ Not assessed √ / O Core taxa in dataset 1/2

* The dataset combining our spacial and temporal data

* * The global survey published by Wu et al.

**Fig. 5.** The putative functions (identified by MiDAS 3 database) of 47 deterministic-dominated bins. The two right-most columns represent the relationships between core taxa and deterministic-dominated bins. AOB, Ammonium oxidizing bacteria; NOB, Nitrite oxidizing bacteria; PAO, Phosphorus accumulating organisms; GAO, Glycogen accumulating organisms.

creased the density of connections in the influent community and created more complex network patterns. Moreover, the topological parameters of the influent networks (Tables 1, 2) changed dramatically compared to those of the AS networks. Studies have indicated that nutrients are important drivers of network structures in microbiological systems (Foster et al., 2012; Zhang et al., 2020). Therefore, changes in environmental conditions, such as COD concentration, can contribute to the dynamics of network structure. Considering that the influent COD concentration varied greatly in different seasons (figure S1), it is not difficult to understand that the structure of influent networks also changed greatly with the seasons.

The AS networks had more stable seasonal topological parameters over time than the influent networks (Tables 1 and 2), which may be related to the stable function of the AS community over time. Interestingly, the network had smaller but more numerous modules in summer and autumn, and more complex modules in spring and winter (Fig. 6). In networks, a module is a group of OTUs that are highly self-connected, but has much fewer connections with OTUs outside the group (Deng et al., 2012). Previous studies indicated that microbes within the same module may perform similar functions. From the perspective of network topological structure, more “small modules” could make the network more stable if they could work simultaneously (Deng et al., 2012; Zhang et al., 2020). The results were reasonable given that nutrients were important drivers of network structures (Shi et al., 2016; Zhang et al., 2020). The seasonal patterns of AS network modules could be a result of varying COD concentrations (i.e., nutrients)

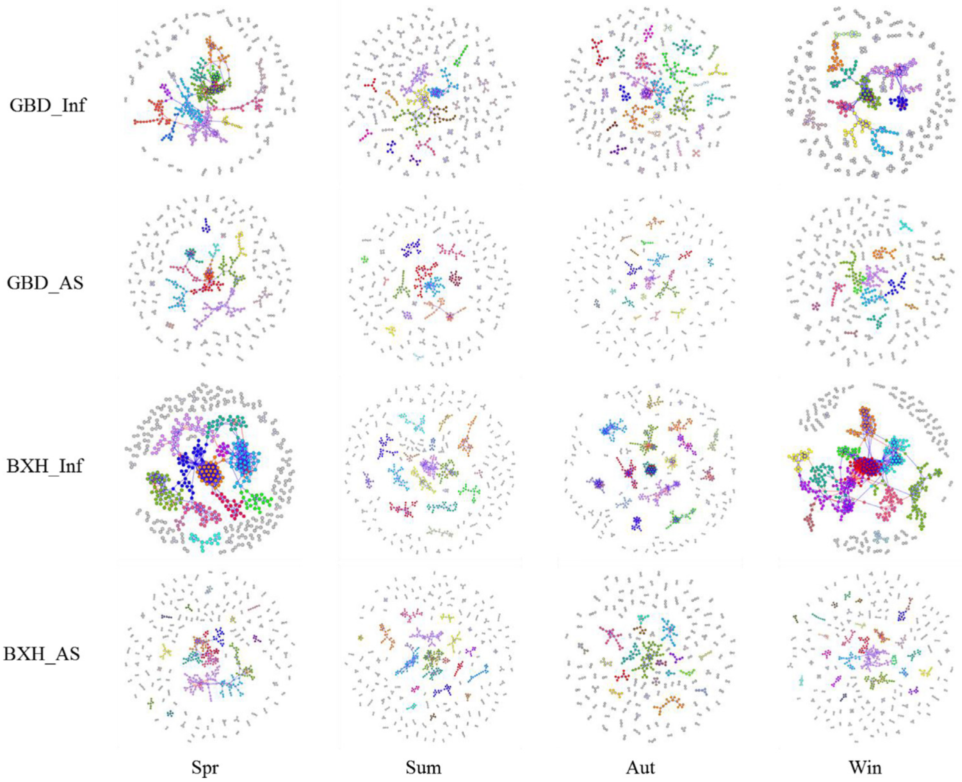

**Fig. 6.** Succession of influent and activated sludge networks in four seasons. The nodes represent OTUs, and the links indicate significant correlation. The modules are randomly colored, and the modules with less than 5 nodes are colored gray. "GBD" and "BXH" represent two different full-scale WWTPs; "Inf" and "AS" represent influent and activated sludge, respectively. "Spr", "Sum", "Aut" and "Win" represent spring, summer, autumn, and winter, respectively.

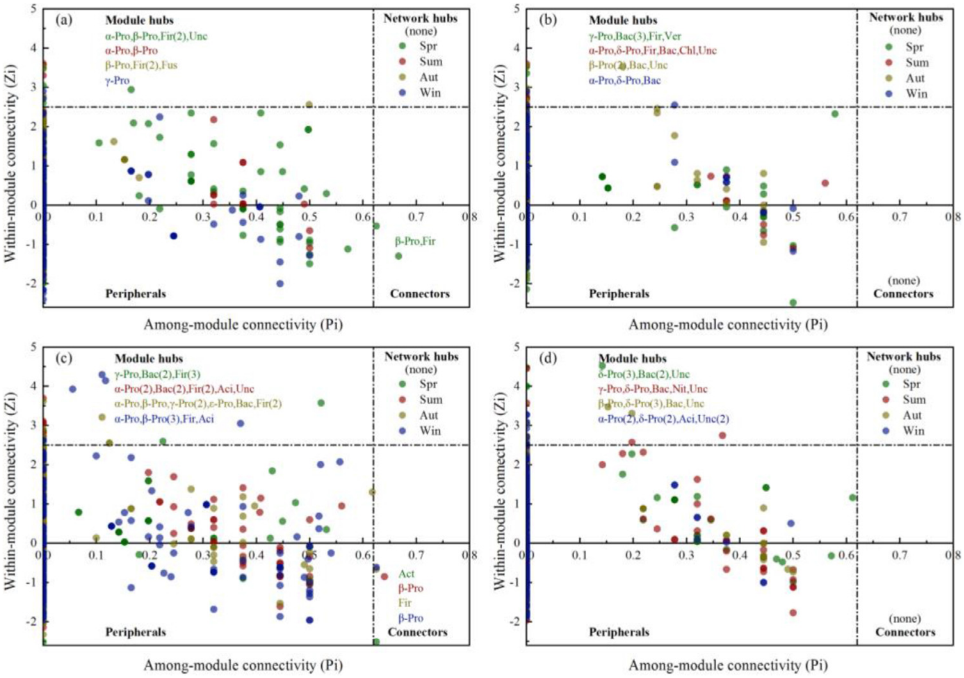

**Fig. 7.** Classification of nodes to identify putative keystone taxa within networks, a) GBD influent; b) GBD activated sludge; c) BXH influent; d) BXH activated slduge. The phylogenetic affiliations of the hubs and connectors are listed on the plot using the following abbreviations: $\alpha$-Pro, *Alphaproteobacteria*; $\beta$-Pro, *Betaproteobacteria*; $\gamma$-Pro, *Gammaproteobacteria*; $\delta$-Pro, *Deltaproteobacteria*; $\varepsilon$-Pro, *Epsilonproteobacteria*; Bac, *Bacteroidetes*; Fir, *Firmicutes*; Fus, *Fusobacteria*; Ver, *Verrucomicrobia*; Chl, *Chlamydiae*; Aci, *Acidobacteria*; Nit, *Nitrospirae*; Unc, Unclassified. The number in parentheses following the taxa information indicates the occurrence number. "Spr", "Sum", "Aut" and "Win" represent spring, summer, autumn, and winter, respectively.

**Table 1**
Topological properties of the constructed molecular ecological networks in GBD. “Inf” and “AS” represent influent and activated sludge, respectively. “Spr”, “Sum”, “Aut” and “Win” represent spring, summer, autumn, and winter, respectively.

| Topological properties | GBD_Inf_Spr | GBD_Inf_Sum | GBD_Inf_Aut | GBD_Inf_Win | GBD_AS_Spr | GBD_AS_Sum | GBD_AS_Aut | GBD_AS_Win |
|---|---|---|---|---|---|---|---|---|
| Average Connectivity | 3.238 | 2.128 | 2.393 | 3.482 | 2.472 | 2.174 | 1.933 | 1.722 |
| Average clustering coefficient (avgCC) | 0.256 | 0.242 | 0.290 | 0.398 | 0.248 | 0.205 | 0.198 | 0.139 |
| Average path distance (GD) | 8.873 | 6.061 | 3.163 | 8.801 | 11.026 | 7.355 | 5.263 | 9.968 |
| Geodesic efficiency (E) | 0.162 | 0.274 | 0.449 | 0.200 | 0.155 | 0.241 | 0.302 | 0.206 |
| Harmonic geodesic distance (HD) | 6.162 | 3.650 | 2.228 | 5.006 | 6.434 | 4.144 | 3.312 | 4.862 |
| Centralization of degree (CD) | 0.055 | 0.019 | 0.039 | 0.030 | 0.042 | 0.030 | 0.027 | 0.013 |
| Centralization of betweenness (CB) | 0.124 | 0.017 | 0.007 | 0.058 | 0.104 | 0.023 | 0.011 | 0.024 |
| Centralization of stress centrality (CS) | 0.627 | 0.165 | 0.010 | 420.796 | 1.516 | 0.092 | 0.024 | 0.062 |
| Centralization of eigenvector centrality (CE) | 0.325 | 0.316 | 0.281 | 0.248 | 0.281 | 0.336 | 0.456 | 0.405 |
| Density (D) | 0.006 | 0.005 | 0.005 | 0.008 | 0.005 | 0.005 | 0.004 | 0.004 |
| Reciprocity | 1 | 1 | 1 | 1 | 1 | 1 | 1 | 1 |
| Transitivity (Trans) | 0.545 | 0.560 | 0.606 | 0.708 | 0.630 | 0.531 | 0.419 | 0.335 |
| Connectedness (Con) | 0.420 | 0.050 | 0.027 | 0.139 | 0.154 | 0.066 | 0.043 | 0.055 |
| Efficiency | 0 | 0.939 | 0.869 | 0.957 | 0.977 | 0.953 | 0.940 | 0.961 |
| Hierarchy | 0 | 0 | 0 | 0 | 0 | 0 | 0 | 0 |
| Lubness | 1 | 1 | 1 | 1 | 1 | 1 | 1 | 1 |
| Modularity(fast_greedy) | 0.829 | 0.934 | 0.932 | 0.891 | 0.911 | 0.936 | 0.948 | 0.923 |

**Table 2**
Topological properties of the constructed molecular ecological networks in BXH. “Inf” and “AS” represent influent and activated sludge, respectively. “Spr”, “Sum”, “Aut” and “Win” represent spring, summer, autumn, and winter, respectively.

| Topological properties | BXH_Inf_Spr | BXH_Inf_Sum | BXH_Inf_Aut | BXH_Inf_Win | BXH_AS_Spr | BXH_AS_Sum | BXH_AS_Aut | BXH_AS_Win |
|---|---|---|---|---|---|---|---|---|
| Average Connectivity | 4.864 | 2.627 | 4.319 | 6.210 | 2.301 | 2.439 | 2.336 | 2.196 |
| Average clustering coefficient (avgCC) | 0.401 | 0.322 | 0.393 | 0.451 | 0.253 | 0.309 | 0.262 | 0.309 |
| Average path distance (GD) | 4.919 | 6.374 | 9.320 | 6.468 | 5.963 | 6.923 | 6.574 | 5.184 |
| Geodesic efficiency (E) | 0.288 | 0.222 | 0.180 | 0.206 | 0.243 | 0.221 | 0.244 | 0.309 |
| Harmonic geodesic distance (HD) | 3.470 | 4.498 | 5.565 | 4.846 | 4.113 | 4.523 | 4.096 | 3.239 |
| Centralization of degree (CD) | 0.062 | 0.014 | 0.023 | 0.059 | 0.026 | 0.022 | 0.021 | 0.014 |
| Centralization of betweenness (CB) | 0.048 | 0.015 | 0.052 | 0.146 | 0.024 | 0.019 | 0.018 | 0.010 |
| Centralization of stress centrality (CS) | 0.483 | 0.399 | 115.125 | 13.766 | 0.246 | 0.467 | 0.336 | 0.027 |
| Centralization of eigenvector centrality (CE) | 0.186 | 0.333 | 0.214 | 0.187 | 0.366 | 0.340 | 0.332 | 0.345 |
| Density (D) | 0.009 | 0.003 | 0.006 | 0.010 | 0.004 | 0.003 | 0.004 | 0.003 |
| Reciprocity | 1 | 1 | 1 | 1 | 1 | 1 | 1 | 1 |
| Transitivity (Trans) | 0.753 | 0.453 | 0.790 | 0.665 | 0.448 | 0.486 | 0.506 | 0.467 |
| Connectedness (Con) | 0.123 | 0.084 | 0.144 | 0.440 | 0.076 | 0.079 | 0.060 | 0.034 |
| Efficiency | 0.941 | 0.971 | 0.967 | 0.980 | 0.966 | 0.970 | 0.956 | 0.932 |
| Hierarchy | 0 | 0 | 0 | 0 | 0 | 0 | 0 | 0 |
| Lubness | 1 | 1 | 1 | 1 | 1 | 1 | 1 | 1 |
| Modularity(fast_greedy) | 0.833 | 0.928 | 0.920 | 0.774 | 0.914 | 0.931 | 0.943 | 0.921 |

across the sampling time. In fact, our results indicated that the COD concentrations of GBD ($P < 0.01$) and BXH ($P < 0.02$) were significantly higher in spring and winter than in summer and autumn. Thus, these variations may induce more complex network structures in spring and winter. Altogether, the results here reported the undocumented seasonal dynamics of network topological parameters of long-term, intensively sampled influent and AS community from full-scale WWTPs, and demonstrated that the AS network structures could be more stable in summer and autumn.

Different nodes played distinct roles in the network developed from microbial abundance data. Previous studies indicated that keystone taxa possess disproportionately more important roles in maintaining network structure than other microorganisms in a network, and the disappearance of these putative keystone taxa may cause networks to disassemble (Shi et al., 2016; Faust and Raes 2012). As shown in Fig. 7, some OTUs were identified as module hubs or connectors in these ecological networks. Briefly, most of these keystone taxa were affiliated to Proteobacteria, Firmicutes, and Bacteroidetes. More detailed taxonomic information was listed in table S22. We found that only two identified keystone taxa repeatedly appeared, and no taxa acted as either a module hub or connector in different networks as the environmental conditions changed over time. These results support the context dependency theory (Power et al., 1996), which means that the keystone taxa can only play crucial roles under certain environmental conditions. Besides, the AS system is considered to be a highly functional redundant system (Vuono et al., 2015; Zhang et al., 2020); thus, different microorganisms may play the same ecological role over time, which may explain the unique keystone taxa detected in different AS networks. Interestingly, we found that the Shannon-Wiener index was significantly negatively correlated with network connectivity (links) in both influent and AS samples (Figure S9). We assume that the lower temperature could act as a strong environmental filter for community assembly. Thus, in spring and winter, lower temperature would promote the development of niches populated by dominant microorganisms, which would lead to decreased diversity and more complex co-occurrence patterns over time due to shared niches. The negatively correlated relationship between diversity and network connectivity highlights the significance of investigating co-occurrence among microorganisms, as they are important dimensions of community organization uncaptured by univariate diversity metrics (Shi et al., 2016; Zhou et al., 2010).

## 4. Conclusion

The analysis of the microbial community of 89 influent and 103 AS time-series samples from two full-scale WWTPs led to the following conclusions: the microbial community diversity and composition in the influent fluctuated substantially with season, while those in the AS had a relatively more stable pattern throughout the year. Firmicutes, Bacteroidetes, Beta-, Gamma-, and Epsilonproteobacteria were the most dominant phyla (or classes) in influent samples, while Alpha-, Beta-, Gamma-, Delta-proteobacteria, Actinobacteria, Acidobacteria, Chloroflexi and Nitrospirae predominated in AS samples. Drift accounted for the largest proportion of the phylogenetic group based assembly mechanisms (52.8%), while homogeneous selection (18.2%) was the most important deterministic process. Deterministic processes dominated in 47 microbial groups (bins), which were also found (~40%) in the AS core taxa dataset. Moreover, the results suggested that *Nitrospira* were more susceptible to stochastic processes in winter, which may provide a possible explanation for nitrification failure in winter. In addition, network analysis results suggested that the network structure of the AS community could be more stable in summer and autumn. There were no identical keystone taxa found in different networks, which supported the context dependency theory. Network complexity was negatively correlated with diversity, indicating that community organization was not captured by univariate diversity metrics.

## Declaration of Competing Interest

The authors declare that they have no known competing financial interests or personal relationships that could have appeared to influence the work reported in this paper.

## Acknowledgment

This study was supported by National Science Foundation of China (No. 52070109). And, C. Sun wants to thank China Scholarship Council (CSC grant #201906210143).

## Supplementary materials

Supplementary material associated with this article can be found, in the online version, at doi:10.1016/j.watres.2021.117295.

## References

Chen, Y.W., Wang, C., Dong, S.Y., Jiang, L., Shi, Y., Li, X.D., Zou, W.T., Tan, Z.L., 2019. Microbial community assembly in detergent wastewater treatment bioreactors: influent rather than inoculum source plays a more important role. Bioresour. Technol. 287, 9.

ChineseNEPA, 2002. Water and Wastewater Monitoring Methods. Chinese Environmental Science Publishing House, Beijing.

Daims, H., Nielsen, J.L., Nielsen, P.H., Schleifer, K.H., Wagner, M., 2001. In situ characterization of Nitrospira-like nitrite oxidizing bacteria active in wastewater treatment plants. Appl. Environ. Microbiol. 67 (11), 5273–5284.

Deng, Y., Jiang, Y.H., Yang, Y.F., He, Z.L., Luo, F., Zhou, J.Z., 2012. Molecular ecological network analyses. BMC Bioinformatics 13, 20.

Dixon, P., 2003. VEGAN, a package of R functions for community ecology. J. Vegetat. Sci. 14 (6), 927–930.

Falk, M.W., Song, K.G., Matiasek, M.G., Wuertz, S., 2009. Microbial community dynamics in replicate membrane bioreactors - natural reproducible fluctuations. Water Res. 43 (3), 842–852.

Faust, K., Raes, J., 2012. Microbial interactions: from networks to models. Nat. Rev. Microbiol. 10 (8), 538–550.

Flowers, J.J., Cadkin, T.A., McMahon, K.D., 2013. Seasonal bacterial community dynamics in a full-scale enhanced biological phosphorus removal plant. Water Res. 47 (19), 7019–7031.

Foster, E.A., Franks, D.W., Morrell, L.J., Balcomb, K.C., Parsons, K.M., van Ginneken, A., Croft, D.P., 2012. Social network correlates of food availability in an endangered population of killer whales, Orcinus orca. Anim. Behav. 83 (3), 731–736.

Fuhrman, J.A., Hewson, I., Schwalbach, M.S., Steele, J.A., Brown, M.V., Naeem, S., 2006. Annually reoccurring bacterial communities are predictable from ocean conditions. Proc. Natl. Acad. Sci. U.S.A. 103 (35), 13104–13109.

Ginige, M.P., Keller, J., Blackall, L.L., 2005. Investigation of an acetate-fed denitrifying microbial community by stable isotope probing, full-cycle rRNA analysis, and fluorescent in situ hybridization-microautoradiography. Appl. Environ. Microbiol. 71 (12), 8683–8691.

Griffin, J.S., Wells, G.F., 2017. Regional synchrony in full-scale activated sludge bioreactors due to deterministic microbial community assembly. Isme J. 11 (2), 500–511.

Jiang, C., Peces, M., Andersen, M.H., Kucheryavskiy, S., Nierychlo, M., Yashiro, E., Andersen, K.S., Kirkegaard, R.H., Hao, L., Hogh, J., Hansen, A.A., Dueholm, M.S., Nielsen, P.H., 2021. Characterizing the growing microorganisms at species level in 46 anaerobic digesters at Danish wastewater treatment plants: a six-year survey on microbial community structure and key drivers. Water Res. 193.

Jiang, X.T., Ye, L., Ju, F., Li, B., Ma, L.P., Zhang, T., 2018a. Temporal dynamics of activated sludge bacterial communities in two diversity variant full-scale sewage treatment plants. Appl. Microbiol. Biotechnol. 102 (21), 9379–9388.

Jiang, X.T., Ye, L., Ju, F., Wang, Y.L., Zhang, T., 2018b. Toward an intensive longitudinal understanding of activated sludge bacterial assembly and dynamics. Environ. Sci. Technol. 52 (15), 8224–8232.

Johnston, J., Behrens, S., 2020. Seasonal dynamics of the activated sludge microbiome in sequencing batch reactors, assessed using 16S rRNA transcript amplicon sequencing. Appl. Environ. Microbiol. 86 (19).

Johnston, J., LaPara, T., Behrens, S., 2019. Composition and dynamics of the activated sludge microbiome during seasonal nitrification failure. Sci. Rep. 9, 15.

Jousset, A., Bienhold, C., Chatzinotas, A., Gallien, L., Gobet, A., Kurm, V., Kusel, K., Rillig, M.C., Rivett, D.W., Salles, J.F., van der Heijden, M.G.A., Youssef, N.H., Zhang, X.W., Wei, Z., Hol, W.H.G., 2017. Where less may be more: how the rare biosphere pulls ecosystems strings. Isme J. 11 (4), 853–862.

Ju, F., Guo, F., Ye, L., Xia, Y., Zhang, T., 2014. Metagenomic analysis on seasonal microbial variations of activated sludge from a full-scale wastewater treatment plant over 4 years. Environ. Microbiol. Rep. 6 (1), 80–89.

Ju, F., Zhang, T., 2015. Bacterial assembly and temporal dynamics in activated sludge of a full-scale municipal wastewater treatment plant. Isme J. 9 (3), 683–695.

Krzywinski, M., Schein, J., Birol, I., Connors, J., Gascoyne, R., Horsman, D., Jones, S.J., Marra, M.A., 2009. Circos: an information aesthetic for comparative genomics. Genome Res. 19 (9), 1639–1645.

Larsen, P., Nielsen, J.L., Otzenj, D., Nielsen, P.H., 2008. Amyloid-like adhesins produced by floc-forming and filamentous bacteria in activated sludge. Appl. Environ. Microbiol. 74 (5), 1517–1526.

Liu, F., Hu, X.M., Zhao, X., Guo, H.X., Zhao, Y., 2019. Microbial community structures' response to seasonal variation in a full-scale municipal wastewater treatment plant. Environ. Eng. Sci. 36 (2), 172–179.

Martin, C., Vanrolleghem, P.A., 2014. Analysing, completing, and generating influent data for WWTP modelling: a critical review. Environ. Model. Softw. 60, 188–201.

McIlroy, S.J., Starnawska, A., Starnawski, P., Saunders, A.M., Nierychlo, M., Nielsen, P.H., Nielsen, J.L., 2016. Identification of active denitrifiers in full-scale nutrient removal wastewater treatment systems. Environ. Microbiol. 18 (1), 50–64.

McLellan, S.L., Huse, S.M., Mueller-Spitz, S.R., Andreishcheva, E.N., Sogin, M.L., 2010. Diversity and population structure of sewage-derived microorganisms in wastewater treatment plant influent. Environ. Microbiol. 12 (2), 378–392.

Nierychlo, M., Andersen, K.S., Xu, Y., Green, N., Jiang, C., Albertsen, M., Dueholm, M.S., Nielsen, P.H., 2020. MiDAS 3: an ecosystem-specific reference database, taxonomy and knowledge platform for activated sludge and anaerobic digesters reveals species-level microbiome composition of activated sludge. Water Res. 182.

Ning, D., Yuan, M., Wu, L., Zhang, Y., Guo, X., Zhou, X., Yang, Y., Arkin, A.P., Firestone, M.K., Zhou, J., 2020. A quantitative framework reveals ecological drivers of grassland microbial community assembly in response to warming. Nat. Commun. 11 (1).

Ofiteru, I.D., Lunn, M., Curtis, T.P., Wells, G.F., Criddle, C.S., Francis, C.A., Sloan, W.T., 2010. Combined niche and neutral effects in a microbial wastewater treatment community. Proc. Natl. Acad. Sci. U.S.A. 107 (35), 15345–15350.

Petrovski, S., Rice, D.T.F., Batinovic, S., Nittami, T., Seviour, R.J., 2020. The community compositions of three nitrogen removal wastewater treatment plants of different configurations in Victoria, Australia, over a 12-month operational period. Appl. Microbiol. Biotechnol. 104 (22), 9839–9852.

Power, M.E., Tilman, D., Estes, J.A., Menge, B.A., Bond, W.J., Mills, L.S., Daily, G., Castilla, J.C., Lubchenco, J., Paine, R.T., 1996. Challenges in the quest for keystones. Bioscience 46 (8), 609–620.

Saunders, A.M., Albertsen, M., Vollertsen, J., Nielsen, P.H., 2016. The activated sludge ecosystem contains a core community of abundant organisms. Isme J. 10 (1), 11–20.

Shade, A., Kent, A.D., Jones, S.E., Newton, R.J., Triplett, E.W., McMahon, K.D., 2007. Interannual dynamics and phenology of bacterial communities in a eutrophic lake. Limnol. Oceanogr. 52 (2), 487–494.

Shi, S.J., Nuccio, E.E., Shi, Z.J., He, Z.L., Zhou, J.Z., Firestone, M.K., 2016. The interconnected rhizosphere: high network complexity dominates rhizosphere assemblages. Ecol. Lett. 19 (8), 926–936.

Sun, C., Zhang, B., Chen, Z., Qin, W., Wen, X., 2020. Sludge retention time affects the microbial community structure: a large-scale sampling of aeration tanks throughout China. Environ. Pollution, 114140.

Tilman, D., 2004. Niche tradeoffs, neutrality, and community structure: a stochastic theory of resource competition, invasion, and community assembly. Proc. Natl. Acad. Sci. U.S.A. 101 (30), 10854–10861.

Vuono, D.C., Benecke, J., Henkel, J., Navidi, W.C., Cath, T.Y., Munakata-Marr, J., Spear, J.R., Drewes, J.E., 2015. Disturbance and temporal partitioning of the activated sludge metacommunity. Isme J. 9 (2), 425–435.

Wagner, M., Loy, A., 2002. Bacterial community composition and function in sewage treatment systems. Curr. Opin. Biotechnol. 13 (3), 218–227.

Wells, G.F., Park, H.D., Eggleston, B., Francis, C.A., Criddle, C.S., 2011. Fine-scale bacterial community dynamics and the taxa-time relationship within a full-scale activated sludge bioreactor. Water Res. 45 (17), 5476–5488.

Wu, L.W., Ning, D.L., Zhang, B., …., Tiedje, J.M., He, Q., Curtis, T.P., Stahl, D.A., Alvarez-Cohen, L., Rittmann, B.E., Wen, X.H., Zhou, J.Z., …, Brown, M., Global Water Microbiome, C., 2019. Global diversity and biogeography of bacterial communities in wastewater treatment plants. Nat. Microbiol. 4 (7), 1183–1195.

Xia, Y., Wen, X.H., Zhang, B., Yang, Y.F., 2018. Diversity and assembly patterns of activated sludge microbial communities: a review. Biotechnol. Adv. 36 (4), 1038–1047.

Zhang, B., Ning, D., Yang, Y., Van Nostrand, J.D., Zhou, J., Wen, X., 2020. Biodegradability of wastewater determines microbial assembly mechanisms in full-scale wastewater treatment plants. Water Res. 169, 115276.

Zhang, B., Yu, Q.W., Yan, G.Q., Zhu, H.B., Xu, X.Y., Zhu, L., 2018. Seasonal bacterial community succession in four typical wastewater treatment plants: correlations between core microbes and process performance. Sci. Rep. 8, 11.

Zheng, W.L., Wen, X.H., 2019. How exogenous influent communities and environmental conditions affect activated sludge communities in the membrane bioreactor of a wastewater treatment plant. Sci. Total Environ. 692, 622–630.

Zheng, W.L., Wen, X.H., Zhang, B., Qiu, Y., 2019. Selective effect and elimination of antibiotics in membrane bioreactor of urban wastewater treatment plant. Sci. Total Environ. 646, 1293–1303.

Zhou, J.Z., Deng, Y., Luo, F., He, Z.L., Tu, Q.C., Zhi, X.Y., 2010. Functional molecular ecological networks. MBio 1 (4), 10.

Zhou, J.Z., Ning, D.L., 2017. Stochastic community assembly: does it matter in microbial ecology? Microbiol. Mol. Biol. Rev. 81 (4), 32.